BABAR-CONF-04/027
SLAC-PUB-10631
August, 2004

Measurement of the $D_{sJ}^*(2317)^+$ and $D_{sJ}(2460)^+$ Properties in $e^+e^- \to c\overline{c}$ Production

The *BABAR* Collaboration

February 7, 2008

Abstract

The properties of the $D_{sJ}^*(2317)^+$ and $D_{sJ}(2460)^+$ mesons are studied using 125 fb^{-1} of $e^+e^- \to c\overline{c}$ data collected by the BaBar experiment. Preliminary mass estimates of [2318.9 $\pm$ 0.3 (stat.) $\pm$ 0.9 (syst.)] MeV/c^2 and [2459.4 $\pm$ 0.3 (stat.) $\pm$ 1.0 (syst.)] MeV/c^2 are obtained. Searches are performed for the decay to the D_s^+ meson along with one or more π^0, π^+, or γ particles. A search is also performed for neutral and doubly-charged partners.

Submitted to the 32$^{\text{nd}}$ International Conference on High-Energy Physics, ICHEP 04,
16 August—22 August 2004, Beijing, China

Stanford Linear Accelerator Center, Stanford University, Stanford, CA 94309

Work supported in part by Department of Energy contract DE-AC03-76SF00515.

The *BABAR* Collaboration,

B. Aubert, R. Barate, D. Boutigny, F. Couderc, J.-M. Gaillard, A. Hicheur, Y. Karyotakis, J. P. Lees, V. Tisserand, A. Zghiche

Laboratoire de Physique des Particules, F-74941 Annecy-le-Vieux, France

A. Palano, A. Pompili

Università di Bari, Dipartimento di Fisica and INFN, I-70126 Bari, Italy

J. C. Chen, N. D. Qi, G. Rong, P. Wang, Y. S. Zhu

Institute of High Energy Physics, Beijing 100039, China

G. Eigen, I. Ofte, B. Stugu

University of Bergen, Inst. of Physics, N-5007 Bergen, Norway

G. S. Abrams, A. W. Borgland, A. B. Breon, D. N. Brown, J. Button-Shafer, R. N. Cahn, E. Charles, C. T. Day, M. S. Gill, A. V. Gritsan, Y. Groysman, R. G. Jacobsen, R. W. Kadel, J. Kadyk, L. T. Kerth, Yu. G. Kolomensky, G. Kukartsev, G. Lynch, L. M. Mir, P. J. Oddone, T. J. Orimoto, M. Pripstein, N. A. Roe, M. T. Ronan, V. G. Shelkov, W. A. Wenzel

Lawrence Berkeley National Laboratory and University of California, Berkeley, CA 94720, USA

M. Barrett, K. E. Ford, T. J. Harrison, A. J. Hart, C. M. Hawkes, S. E. Morgan, A. T. Watson

University of Birmingham, Birmingham, B15 2TT, United Kingdom

M. Fritsch, K. Goetzen, T. Held, H. Koch, B. Lewandowski, M. Pelizaeus, M. Steinke

Ruhr Universität Bochum, Institut für Experimentalphysik 1, D-44780 Bochum, Germany

J. T. Boyd, N. Chevalier, W. N. Cottingham, M. P. Kelly, T. E. Latham, F. F. Wilson

University of Bristol, Bristol BS8 1TL, United Kingdom

T. Cuhadar-Donszelmann, C. Hearty, N. S. Knecht, T. S. Mattison, J. A. McKenna, D. Thiessen

University of British Columbia, Vancouver, BC, Canada V6T 1Z1

A. Khan, P. Kyberd, L. Teodorescu

Brunel University, Uxbridge, Middlesex UB8 3PH, United Kingdom

A. E. Blinov, V. E. Blinov, V. P. Druzhinin, V. B. Golubev, V. N. Ivanchenko, E. A. Kravchenko, A. P. Onuchin, S. I. Serednyakov, Yu. I. Skovpen, E. P. Solodov, A. N. Yushkov

Budker Institute of Nuclear Physics, Novosibirsk 630090, Russia

D. Best, M. Bruinsma, M. Chao, I. Eschrich, D. Kirkby, A. J. Lankford, M. Mandelkern, R. K. Mommsen, W. Roethel, D. P. Stoker

University of California at Irvine, Irvine, CA 92697, USA

C. Buchanan, B. L. Hartfiel

University of California at Los Angeles, Los Angeles, CA 90024, USA

S. D. Foulkes, J. W. Gary, B. C. Shen, K. Wang

University of California at Riverside, Riverside, CA 92521, USA

D. del Re, H. K. Hadavand, E. J. Hill, D. B. MacFarlane, H. P. Paar, Sh. Rahatlou, V. Sharma

University of California at San Diego, La Jolla, CA 92093, USA

J. W. Berryhill, C. Campagnari, B. Dahmes, O. Long, A. Lu, M. A. Mazur, J. D. Richman, W. Verkerke

University of California at Santa Barbara, Santa Barbara, CA 93106, USA

T. W. Beck, A. M. Eisner, C. A. Heusch, J. Kroseberg, W. S. Lockman, G. Nesom, T. Schalk, B. A. Schumm, A. Seiden, P. Spradlin, D. C. Williams, M. G. Wilson

University of California at Santa Cruz, Institute for Particle Physics, Santa Cruz, CA 95064, USA

J. Albert, E. Chen, G. P. Dubois-Felsmann, A. Dvoretskii, D. G. Hitlin, I. Narsky, T. Piatenko, F. C. Porter, A. Ryd, A. Samuel, S. Yang

California Institute of Technology, Pasadena, CA 91125, USA

S. Jayatilleke, G. Mancinelli, B. T. Meadows, M. D. Sokoloff

University of Cincinnati, Cincinnati, OH 45221, USA

T. Abe, F. Blanc, P. Bloom, S. Chen, W. T. Ford, U. Nauenberg, A. Olivas, P. Rankin, J. G. Smith, J. Zhang, L. Zhang

University of Colorado, Boulder, CO 80309, USA

A. Chen, J. L. Harton, A. Soffer, W. H. Toki, R. J. Wilson, Q. Zeng

Colorado State University, Fort Collins, CO 80523, USA

D. Altenburg, T. Brandt, J. Brose, M. Dickopp, E. Feltresi, A. Hauke, H. M. Lacker, R. Müller-Pfefferkorn, R. Nogowski, S. Otto, A. Petzold, J. Schubert, K. R. Schubert, R. Schwierz, B. Spaan, J. E. Sundermann

Technische Universität Dresden, Institut für Kern- und Teilchenphysik, D-01062 Dresden, Germany

D. Bernard, G. R. Bonneaud, F. Brochard, P. Grenier, S. Schrenk, Ch. Thiebaux, G. Vasileiadis, M. Verderi

Ecole Polytechnique, LLR, F-91128 Palaiseau, France

D. J. Bard, P. J. Clark, D. Lavin, F. Muheim, S. Playfer, Y. Xie

University of Edinburgh, Edinburgh EH9 3JZ, United Kingdom

M. Andreotti, V. Azzolini, D. Bettoni, C. Bozzi, R. Calabrese, G. Cibinetto, E. Luppi, M. Negrini, L. Piemontese, A. Sarti

Università di Ferrara, Dipartimento di Fisica and INFN, I-44100 Ferrara, Italy

E. Treadwell

Florida A&M University, Tallahassee, FL 32307, USA

F. Anulli, R. Baldini-Ferroli, A. Calcaterra, R. de Sangro, G. Finocchiaro, P. Patteri, I. M. Peruzzi, M. Piccolo, A. Zallo

Laboratori Nazionali di Frascati dell'INFN, I-00044 Frascati, Italy

A. Buzzo, R. Capra, R. Contri, G. Crosetti, M. Lo Vetere, M. Macri, M. R. Monge, S. Passaggio, C. Patrignani, E. Robutti, A. Santroni, S. Tosi

Università di Genova, Dipartimento di Fisica and INFN, I-16146 Genova, Italy

S. Bailey, G. Brandenburg, K. S. Chaisanguanthum, M. Morii, E. Won

Harvard University, Cambridge, MA 02138, USA

R. S. Dubitzky, U. Langenegger

Universität Heidelberg, Physikalisches Institut, Philosophenweg 12, D-69120 Heidelberg, Germany

W. Bhimji, D. A. Bowerman, P. D. Dauncey, U. Egede, J. R. Gaillard, G. W. Morton, J. A. Nash, M. B. Nikolich, G. P. Taylor

Imperial College London, London, SW7 2AZ, United Kingdom

M. J. Charles, G. J. Grenier, U. Mallik

University of Iowa, Iowa City, IA 52242, USA

J. Cochran, H. B. Crawley, J. Lamsa, W. T. Meyer, S. Prell, E. I. Rosenberg, A. E. Rubin, J. Yi

Iowa State University, Ames, IA 50011-3160, USA

M. Biasini, R. Covarelli, M. Pioppi

Università di Perugia, Dipartimento di Fisica and INFN, I-06100 Perugia, Italy

M. Davier, X. Giroux, G. Grosdidier, A. Höcker, S. Laplace, F. Le Diberder, V. Lepeltier, A. M. Lutz, T. C. Petersen, S. Plaszczynski, M. H. Schune, L. Tantot, G. Wormser

Laboratoire de l'Accélérateur Linéaire, F-91898 Orsay, France

C. H. Cheng, D. J. Lange, M. C. Simani, D. M. Wright

Lawrence Livermore National Laboratory, Livermore, CA 94550, USA

A. J. Bevan, C. A. Chavez, J. P. Coleman, I. J. Forster, J. R. Fry, E. Gabathuler, R. Gamet, D. E. Hutchcroft, R. J. Parry, D. J. Payne, R. J. Sloane, C. Touramanis

University of Liverpool, Liverpool L69 72E, United Kingdom

J. J. Back,[1] C. M. Cormack, P. F. Harrison,[1] F. Di Lodovico, G. B. Mohanty[1]

Queen Mary, University of London, E1 4NS, United Kingdom

C. L. Brown, G. Cowan, R. L. Flack, H. U. Flaecher, M. G. Green, P. S. Jackson, T. R. McMahon, S. Ricciardi, F. Salvatore, M. A. Winter

University of London, Royal Holloway and Bedford New College, Egham, Surrey TW20 0EX, United Kingdom

D. Brown, C. L. Davis

University of Louisville, Louisville, KY 40292, USA

J. Allison, N. R. Barlow, R. J. Barlow, P. A. Hart, M. C. Hodgkinson, G. D. Lafferty, A. J. Lyon, J. C. Williams

University of Manchester, Manchester M13 9PL, United Kingdom

A. Farbin, W. D. Hulsbergen, A. Jawahery, D. Kovalskyi, C. K. Lae, V. Lillard, D. A. Roberts

University of Maryland, College Park, MD 20742, USA

G. Blaylock, C. Dallapiccola, K. T. Flood, S. S. Hertzbach, R. Kofler, V. B. Koptchev, T. B. Moore, S. Saremi, H. Staengle, S. Willocq

University of Massachusetts, Amherst, MA 01003, USA

[1]Now at Department of Physics, University of Warwick, Coventry, United Kingdom

R. Cowan, G. Sciolla, S. J. Sekula, F. Taylor, R. K. Yamamoto

Massachusetts Institute of Technology, Laboratory for Nuclear Science, Cambridge, MA 02139, USA

D. J. J. Mangeol, P. M. Patel, S. H. Robertson

McGill University, Montréal, QC, Canada H3A 2T8

A. Lazzaro, V. Lombardo, F. Palombo

Università di Milano, Dipartimento di Fisica and INFN, I-20133 Milano, Italy

J. M. Bauer, L. Cremaldi, V. Eschenburg, R. Godang, R. Kroeger, J. Reidy, D. A. Sanders, D. J. Summers, H. W. Zhao

University of Mississippi, University, MS 38677, USA

S. Brunet, D. Côté, P. Taras

Université de Montréal, Laboratoire René J. A. Lévesque, Montréal, QC, Canada H3C 3J7

H. Nicholson

Mount Holyoke College, South Hadley, MA 01075, USA

N. Cavallo,[2] F. Fabozzi,[2] C. Gatto, L. Lista, D. Monorchio, P. Paolucci, D. Piccolo, C. Sciacca

Università di Napoli Federico II, Dipartimento di Scienze Fisiche and INFN, I-80126, Napoli, Italy

M. Baak, H. Bulten, G. Raven, H. L. Snoek, L. Wilden

NIKHEF, National Institute for Nuclear Physics and High Energy Physics, NL-1009 DB Amsterdam, The Netherlands

C. P. Jessop, J. M. LoSecco

University of Notre Dame, Notre Dame, IN 46556, USA

T. Allmendinger, K. K. Gan, K. Honscheid, D. Hufnagel, H. Kagan, R. Kass, T. Pulliam, A. M. Rahimi, R. Ter-Antonyan, Q. K. Wong

Ohio State University, Columbus, OH 43210, USA

J. Brau, R. Frey, O. Igonkina, C. T. Potter, N. B. Sinev, D. Strom, E. Torrence

University of Oregon, Eugene, OR 97403, USA

F. Colecchia, A. Dorigo, F. Galeazzi, M. Margoni, M. Morandin, M. Posocco, M. Rotondo, F. Simonetto, R. Stroili, G. Tiozzo, C. Voci

Università di Padova, Dipartimento di Fisica and INFN, I-35131 Padova, Italy

M. Benayoun, H. Briand, J. Chauveau, P. David, Ch. de la Vaissière, L. Del Buono, O. Hamon, M. J. J. John, Ph. Leruste, J. Malcles, J. Ocariz, M. Pivk, L. Roos, S. T'Jampens, G. Therin

Universités Paris VI et VII, Laboratoire de Physique Nucléaire et de Hautes Energies, F-75252 Paris, France

P. F. Manfredi, V. Re

Università di Pavia, Dipartimento di Elettronica and INFN, I-27100 Pavia, Italy

[2]Also with Università della Basilicata, Potenza, Italy

P. K. Behera, L. Gladney, Q. H. Guo, J. Panetta

University of Pennsylvania, Philadelphia, PA 19104, USA

C. Angelini, G. Batignani, S. Bettarini, M. Bondioli, F. Bucci, G. Calderini, M. Carpinelli, F. Forti, M. A. Giorgi, A. Lusiani, G. Marchiori, F. Martinez-Vidal,[3] M. Morganti, N. Neri, E. Paoloni, M. Rama, G. Rizzo, F. Sandrelli, J. Walsh

Università di Pisa, Dipartimento di Fisica, Scuola Normale Superiore and INFN, I-56127 Pisa, Italy

M. Haire, D. Judd, K. Paick, D. E. Wagoner

Prairie View A&M University, Prairie View, TX 77446, USA

N. Danielson, P. Elmer, Y. P. Lau, C. Lu, V. Miftakov, J. Olsen, A. J. S. Smith, A. V. Telnov

Princeton University, Princeton, NJ 08544, USA

F. Bellini, G. Cavoto,[4] R. Faccini, F. Ferrarotto, F. Ferroni, M. Gaspero, L. Li Gioi, M. A. Mazzoni, S. Morganti, M. Pierini, G. Piredda, F. Safai Tehrani, C. Voena

Università di Roma La Sapienza, Dipartimento di Fisica and INFN, I-00185 Roma, Italy

S. Christ, G. Wagner, R. Waldi

Universität Rostock, D-18051 Rostock, Germany

T. Adye, N. De Groot, B. Franek, N. I. Geddes, G. P. Gopal, E. O. Olaiya

Rutherford Appleton Laboratory, Chilton, Didcot, Oxon, OX11 0QX, United Kingdom

R. Aleksan, S. Emery, A. Gaidot, S. F. Ganzhur, P.-F. Giraud, G. Hamel de Monchenault, W. Kozanecki, M. Legendre, G. W. London, B. Mayer, G. Schott, G. Vasseur, Ch. Yèche, M. Zito

DSM/Dapnia, CEA/Saclay, F-91191 Gif-sur-Yvette, France

M. V. Purohit, A. W. Weidemann, J. R. Wilson, F. X. Yumiceva

University of South Carolina, Columbia, SC 29208, USA

D. Aston, R. Bartoldus, N. Berger, A. M. Boyarski, O. L. Buchmueller, R. Claus, M. R. Convery, M. Cristinziani, G. De Nardo, D. Dong, J. Dorfan, D. Dujmic, W. Dunwoodie, E. E. Elsen, S. Fan, R. C. Field, T. Glanzman, S. J. Gowdy, T. Hadig, V. Halyo, C. Hast, T. Hryn'ova, W. R. Innes, M. H. Kelsey, P. Kim, M. L. Kocian, D. W. G. S. Leith, J. Libby, S. Luitz, V. Luth, H. L. Lynch, H. Marsiske, R. Messner, D. R. Muller, C. P. O'Grady, V. E. Ozcan, A. Perazzo, M. Perl, S. Petrak, B. N. Ratcliff, A. Roodman, A. A. Salnikov, R. H. Schindler, J. Schwiening, G. Simi, A. Snyder, A. Soha, J. Stelzer, D. Su, M. K. Sullivan, J. Va'vra, S. R. Wagner, M. Weaver, A. J. R. Weinstein, W. J. Wisniewski, M. Wittgen, D. H. Wright, A. K. Yarritu, C. C. Young

Stanford Linear Accelerator Center, Stanford, CA 94309, USA

P. R. Burchat, A. J. Edwards, T. I. Meyer, B. A. Petersen, C. Roat

Stanford University, Stanford, CA 94305-4060, USA

S. Ahmed, M. S. Alam, J. A. Ernst, M. A. Saeed, M. Saleem, F. R. Wappler

State University of New York, Albany, NY 12222, USA

[3]Also with IFIC, Instituto de Física Corpuscular, CSIC-Universidad de Valencia, Valencia, Spain
[4]Also with Princeton University, Princeton, USA

W. Bugg, M. Krishnamurthy, S. M. Spanier
University of Tennessee, Knoxville, TN 37996, USA

R. Eckmann, H. Kim, J. L. Ritchie, A. Satpathy, R. F. Schwitters
University of Texas at Austin, Austin, TX 78712, USA

J. M. Izen, I. Kitayama, X. C. Lou, S. Ye
University of Texas at Dallas, Richardson, TX 75083, USA

F. Bianchi, M. Bona, F. Gallo, D. Gamba
Università di Torino, Dipartimento di Fisica Sperimentale and INFN, I-10125 Torino, Italy

L. Bosisio, C. Cartaro, F. Cossutti, G. Della Ricca, S. Dittongo, S. Grancagnolo, L. Lanceri, P. Poropat,[5] L. Vitale, G. Vuagnin
Università di Trieste, Dipartimento di Fisica and INFN, I-34127 Trieste, Italy

R. S. Panvini
Vanderbilt University, Nashville, TN 37235, USA

Sw. Banerjee, C. M. Brown, D. Fortin, P. D. Jackson, R. Kowalewski, J. M. Roney, R. J. Sobie
University of Victoria, Victoria, BC, Canada V8W 3P6

H. R. Band, B. Cheng, S. Dasu, M. Datta, A. M. Eichenbaum, M. Graham, J. J. Hollar, J. R. Johnson, P. E. Kutter, H. Li, R. Liu, A. Mihalyi, A. K. Mohapatra, Y. Pan, R. Prepost, P. Tan, J. H. von Wimmersperg-Toeller, J. Wu, S. L. Wu, Z. Yu
University of Wisconsin, Madison, WI 53706, USA

M. G. Greene, H. Neal
Yale University, New Haven, CT 06511, USA

[5]Deceased

1 INTRODUCTION

The $D_{sJ}^*(2317)^+$ meson, discovered by this collaboration [1] and confirmed by others [2, 3, 4], and the $D_{sJ}(2460)^+$ meson, observed by the CLEO collaboration [2] and confirmed by this collaboration [5] and others [3], has reawakened interest in the study of the spectroscopy of charm mesons.

Presented in this paper is an updated, preliminary analysis of these states using 125 fb^{-1} of $e^+e^- \to c\overline{c}$ data collected by the *BABAR* experiment. From this analysis we present new estimates of the $D_{sJ}^*(2317)^+$ and $D_{sJ}(2460)^+$ masses and the branching ratios of $D_{sJ}(2460)^+$ decays to $D_s^+\gamma$ and $D_s^+\pi^+\pi^-$ with respect to its decay to $D_s^+\pi^0\gamma$. In addition, we search for new decays of either meson involving a D_s^+ meson accompanied by π^0 and $\pi^\pm$ mesons and photons. An estimate of the $D_{s1}(2536)^+$ mass is also presented.

These measurements are performed by fitting the invariant mass spectrums of combinations [6] of $D_s^+\pi^0$, $D_s^+\gamma$, $D_s^+\pi^0\gamma$, and $D_s^+\pi^+\pi^-$ particles. Combinations of $D_s^+\pi^+$ and $D_s^+\pi^-$ are also studied in the search for new states. The following two sections of this paper describe those details in common to the entire analysis. The study of each combination is then discussed in their own section. The paper ends with a summary.

2 CANDIDATE SELECTION

This analysis is performed using a 125 fb^{-1} data sample collected on or near the $\Upsilon(4S)$ resonance with the *BABAR* detector at the PEP-II asymmetric-energy e^+e^- storage rings. The *BABAR* detector, a general-purpose, solenoidal, magnetic spectrometer, is described in detail elsewhere [6]. Charged particles were detected and their momenta measured by a combination of a drift chamber (DCH) and silicon vertex tracker (SVT), both operating within a 1.5-T solenoidal magnetic field. A ring-imaging Cherenkov detector (DIRC) is used for charged-particle identification. Photons are detected and measured with a CsI electromagnetic calorimeter (EMC).

All of the final states explored in this analysis involve one D_s^+ candidate decaying to $K^+K^-\pi^+$. A clean sample of $K^\pm$ candidates is obtained using particle identification by requiring a Cherenkov photon yield and angle consistent with the $K^\pm$ hypothesis. This information is augmented with energy loss measurements in the tracking systems. The efficiency of $K^\pm$ identification is approximately 85% in the kinematic range used in this analysis with a $\pi^\pm$ misidentification rate of less than 2%. A similar procedure is used to produce a sample of $\pi^\pm$ candidates.

Each D_s^+ candidate is constructed by combining a K^+K^- candidate pair with a π^+ candidate in a geometrical fit to a common vertex. An acceptable $K^+K^-\pi^+$ candidate must have a fit probability greater than 0.1% and a trajectory consistent with originating from the e^+e^- luminous region. Backgrounds are further suppressed by selecting decays to $\overline{K}^{*0}K^+$ and $\phi\pi^+$. Additional details of this selection procedure can be found elsewhere [1]. Combinations of $K^-K^+\pi^+$ with $1.954 < m(K^+K^-\pi^+) < 1.981$ GeV/c^2 are taken as D_s^+ candidates.

For the purposes of calculating the invariant mass of the various particle combinations in this paper, the energy of each D_s^+ candidate is calculated from the measured momenta and the PDG D_s^+ mass of 1968.5 MeV/c^2 [7]. The uncertainty in this mass (0.6 MeV/c^2) is taken as a systematic uncertainty.

Once a D_s^+ candidate is obtained, a search is performed for all accompanying π^0, γ, and $\pi^\pm$ particles. All energy clusters in the EMC unassociated with charged tracks and consistent with an

[6] Inclusion of charge conjugate states is implied throughout this paper.

electromagnetic shower are considered photon candidates. A candidate π^0 is formed by constraining a pair of photons each with energy greater than 100 MeV to emanate from the intersection of the D_s^+ trajectory with the beam envelope, performing a one-constraint fit to the π^0 mass, and requiring a fit probability greater than 2%.

A given event may yield several acceptable π^0 candidates. For the various final-state samples used in this analysis, we retain only those candidates for which neither photon belongs to another otherwise acceptable π^0 of momentum greater than 150 MeV/c. In a similar fashion, we discard any γ candidate which belongs to the same list of acceptable π^0 candidates.

3 SIMULATION AND CALIBRATION

The efficiency and reconstructed mass distribution of all final-state combinations discussed in this document are derived from detailed simulation based on the Geant4 [8] toolkit, reconstructed with the same algorithms as the data, and passing the same selection requirements. Individual samples of between 120,000 and 240,000 events were generated for each individual signal.

In addition, for the purposes of optimizing candidate selection requirements, a simulated sample corresponding to 30 fb^{-1} of $e^+e^- \to c\overline{c}$ events is used to describe combinatorial background.

Clean samples of $\tau \to \rho\nu$ and $\tau \to \pi\nu$ were studied to validate the accuracy of the simulation of the reconstruction efficiency and energy scale for photon and π^0 candidates. Based on this study, a photon efficiency correction of 1.6% and EMC energy scale corrections of between 0.2% and 0.8% is applied. The remaining systematic uncertainty in the Monte Carlo prediction of neutral efficiency and energy scale is a relative 3% and 1%, respectively.

The reconstruction and selection efficiency of the various final-state combinations studied in this analysis tend to be dependent on the center-of-mass momentum p^* of the $D_{sJ}^*(2317)^+$ and $D_{sJ}(2460)^+$. To minimize any dependence on the p^* distribution assumed in the Monte Carlo, each final-state is restricted to the same minimum p^* value of 3.2 GeV/c^2 (this also serves to remove production from B decay). In addition, a p^* dependent efficiency function derived from Monte Carlo is used to calculate efficiency corrected yields for all decay modes.

Estimates of the tracking efficiency obtained from τ decays and from a comparison of SVT and DCH measurements indicate that the Monte Carlo prediction of $\pi^\pm$ efficiency is, on average, 0.8% too high, with a systematic uncertainty of 1.3%.

4 THE $D_s^+\pi^0$ SYSTEM

To form $D_s^+\pi^0$ combinations, each D_s^+ candidate is combined with one π^0 candidate. The p^* of the resulting combination is required to be greater than 3.2 GeV/c. The corresponding invariant mass distribution is shown in Fig. 1. Signals for $D_{sJ}^*(2317)^+$ and $D_s^*(2112)^+$ are clearly visible.

For the purposes of fitting the $D_s^+\pi^0$ mass spectrum and extracting information on the $D_{sJ}^*(2317)^+$ and $D_{sJ}(2460)^+$ mesons, the $D_s^+\pi^0$ sample is restricted to those π^0 candidates with momentum greater than 400 MeV/c. This momentum requirement is based on an optimization of $Q = \varepsilon/\sqrt{B}$, where ε is the efficiency for the hypothetical decay $D_{sJ}(2460)^+ \to D_s^+\pi^0$, and B is the amount of background as predicted by Monte Carlo. The resulting invariant mass distribution is shown in Fig. 2. As a result of this stricter π^0 momentum requirement, the $D_s^*(2112)^+ \to D_s^+\pi^0$ signal is entirely eliminated.

Estimates of the yield and mass of the $D_{sJ}^*(2317)^+$ are obtained using a unbinned likelihood fit of the $D_s^+\pi^0$ mass spectrum. The lineshape is also used to calculate a limit on the yield from

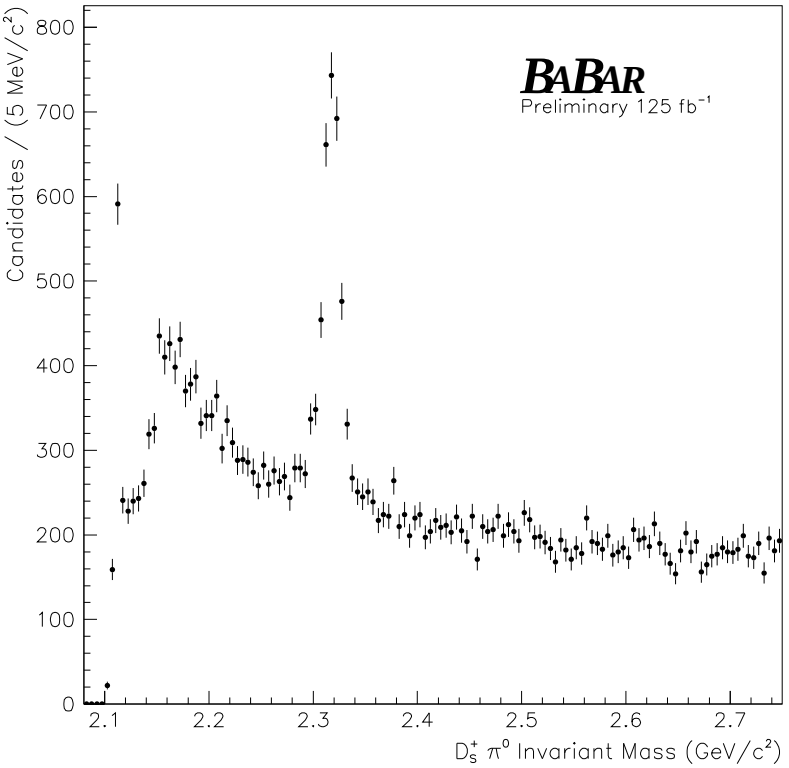

Figure 1: The $D_s^+\pi^0$ invariant mass distribution for candidates with loose π^0 requirements.

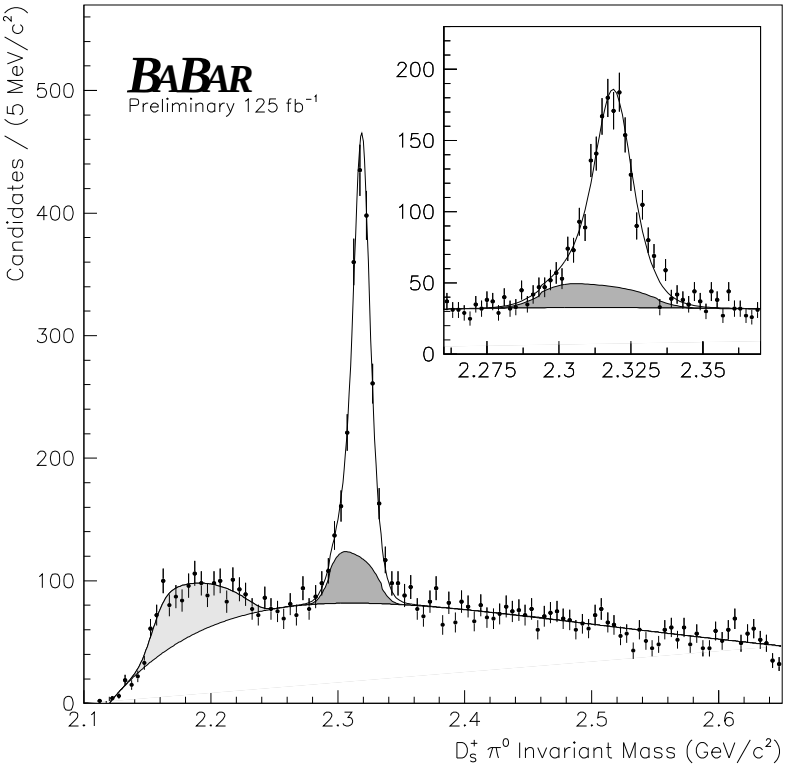

Figure 2: The $D_s^+\pi^0$ invariant mass distribution for candidates that satisfy the requirements discussed in the text. The solid curve is the result of a unbinned likelihood fit. The dark (light) gray region is the contribution from the $D_{sJ}(2460)^+ \to D_s^+\pi^0\gamma$ ($D_s^*(2112)^+ \to D_s^+\gamma$) reflection. The inset is an expanded view near the $D_{sJ}^*(2317)^+$ mass.

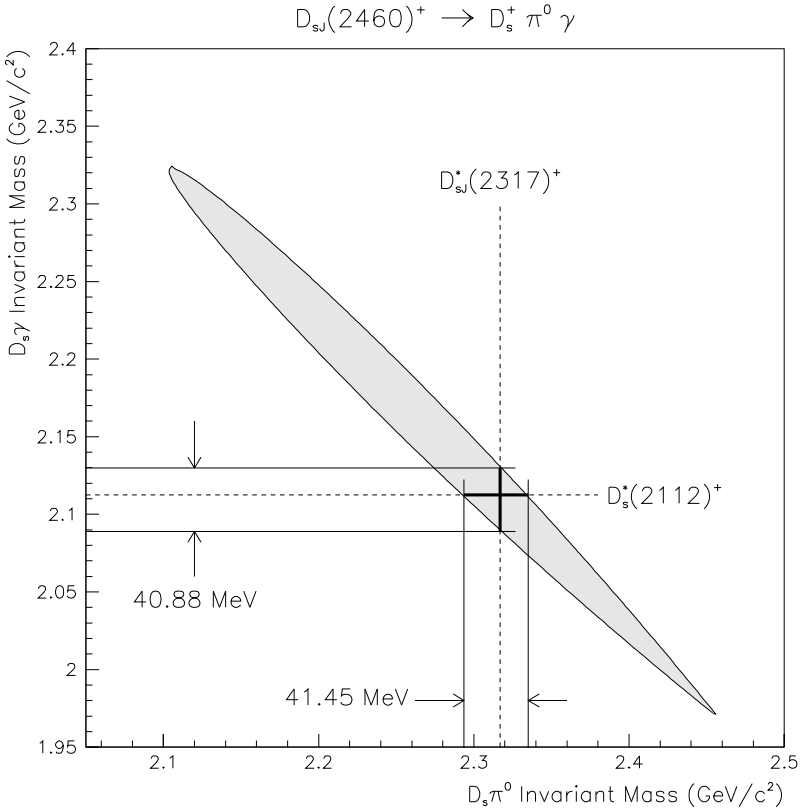

Figure 3: The kinematics of $D_{sJ}(2460)^+ \rightarrow D_s^+\pi^0\gamma$ decay. The shaded area indicates the region of $D_s^+\pi^0$ and $D_s^+\gamma$ mass that is kinematically allowed in the decay of an object of mass 2459.2 MeV/c^2. The lines mark the kinematic space limited to the decay which proceeds through intermediate $D_s^*(2112)^+$ or $D_{sJ}^*(2317)^+$ mesons.

hypothetical $D_{sJ}(2460)^+ \rightarrow D_s^+\pi^0$ decays. The lineshapes of the reconstructed $D_{sJ}^*(2317)^+$ and $D_{sJ}(2460)^+$ mass distributions are obtained from fits to simulated signal events. In both the simulation and in the fit it is assumed that the intrinsic width Γ of both mesons is small enough that this lineshape is not significantly affected.

The background to the $D_{sJ}^*(2317)^+$ comes from unrelated D_s^+ and π^0 (the combinatorial background) and from two types of reflections. One reflection, from $D_s^*(2112)^+ \rightarrow D_s^+\gamma$ decays combined with an unassociated γ to form a fake π^0 candidate, is peaked near the kinematic limit in $D_s^+\pi^0$ mass of 2154.6 MeV/c^2. The second reflection is produced by the D_s^+ and π^0 mesons from $D_{sJ}(2460)^+ \rightarrow D_s^*(2112)^+\pi^0$ decay. Due to a kinematic coincidence, this reflection has a mean mass that is close to the $D_{sJ}^*(2317)^+$ mass and must be accurately determined in order to correctly measure the $D_{sJ}^*(2317)^+$ properties. As shown in Fig. 3, if reconstruction efficiency is uniform, the $D_{sJ}(2460)^+$ reflection would appear as a nearly square function of total width 41.5 MeV/c^2 smeared by resolution. Because of the variation in reconstruction efficiency across the $D_{sJ}(2460)^+$ phase space, the reflection shape is asymmetric. The prediction from $D_{sJ}(2460)^+$ Monte Carlo is used to determine the precise shape.

The likelihood fit to the $D_s^+\pi^0$ mass spectrum is shown in Fig. 2. Whereas the shape and magnitude of the $D_{sJ}(2460)^+$ reflection are fixed to Monte Carlo predictions, the parameters of

the $D_s^*(2112)^+$ reflection and the shape of the combinatorial background are allowed to vary in the fit. The mass and yield of the $D_{sJ}^*(2317)^+$ are determined by shifting the associated lineshape up or down in mass and adjusting the overall amplitude to best match the data. A limit on the yield of the hypothetical $D_{sJ}(2460)^+ \to D_s^+\pi^0$ decay is determined by adjusting the amplitude of the associated lineshape positive or negative to best match the data. The resulting likelihood fit successfully describes the data.

The fit determines (statistical errors only) a $D_{sJ}^*(2317)^+$ mass of $[2318.9 \pm 0.3]$ MeV/c^2 and raw $D_{sJ}^*(2317)^+$ and $D_{sJ}(2460)^+$ yields of 1275 ± 45 and 3 ± 26 mesons.

A systematic uncertainty specific to the fit to the $D_s^+\pi^0$ system is the size of the $D_{sJ}(2460)^+$ reflection. If the likelihood fit is allowed to adjust the size of this reflection to best match the data, the result is a $D_{sJ}^*(2317)^+$ yield 0.5% smaller and a shift in $D_{sJ}^*(2317)^+$ mass that is less than 0.1 MeV/c^2. In addition, various different models of the $D_s^*(2112)^+$ reflection can be used in the fit, in which case variations in the $D_{sJ}^*(2317)^+$ yield of up to 0.4% are observed.

5 THE $D_s^+\gamma$ SYSTEM

To form $D_s^+\gamma$ combinations, each D_s^+ candidate is combined with γ candidates with energy greater than 500 MeV/c. This energy requirement is based on an optimization of $Q' = S/\sqrt{S+B}$, where S is the expected signal size [3] and B is the amount of background as predicted by Monte Carlo for the decay $D_{sJ}(2460)^+ \to D_s^+\gamma$. In addition, any $D_s^+\gamma$ combination with p^* less than 3.2 GeV/c is discarded. The resulting invariant mass distribution is shown in Fig. 4.

For reasons of simplicity, the likelihood fit is restricted to a $D_s^+\gamma$ mass range between 2.15 and 2.85 MeV/c^2. As shown in Fig. 4, there are two structures clearly visible in this spectrum within this range on top of a gradually falling background distribution. The higher mass structure corresponds to the $D_{sJ}(2460)^+$ meson. The likelihood fit uses a signal lineshape determined from signal Monte Carlo. To determine the $D_{sJ}(2460)^+$ mass, the mean value of the signal is allowed to shift. To determine the $D_{sJ}(2460)^+$ yield, the fit determines the amplitude that bests describes the data.

The lower mass structure is a combination of two reflections. The largest reflection is composed of the D_s^+ meson from the decay $D_{sJ}^*(2317)^+ \to D_s^+\pi^0$ combined with one of the photons from the π^0. The second is produced in a similar fashion from $D_{sJ}(2460)^+ \to D_s^+\pi^0\gamma$ decay. The shapes of these two reflections are influenced by the candidate selection requirements and, in particular, the requirement that the γ particle not belong to a π^0 candidate. This interdependency is complex enough that the Monte Carlo simulation fails to adequately reproduce the precise shape of the reflection. For this reason a parameterization of $D_{sJ}^*(2317)^+ \to D_s^+\pi^0$ reflection shape is included as part of the fit. The $D_{sJ}(2460)^+ \to D_s^+\pi^0\gamma$ reflection shape is fixed to the prediction from Monte Carlo.

The kinematics of $D_{sJ}^*(2317)^+ \to D_s^+\pi^0$ decay require that the $D_s^+\gamma$ reflection end at $D_s^+\gamma$ mass of 2.304 MeV/c^2. The lineshape assumed by the likelihood fit respects this limit but includes detector resolution effects that will tend to blur this boundary. Just adjacent to the boundary is where a hypothetical $D_{sJ}^*(2317)^+ \to D_s^+\gamma$ signal would reside. The lineshape of the $D_{sJ}^*(2317)^+$ signal is extracted from signal Monte Carlo. Because of uncertainties in the precise shape of the $D_{sJ}^*(2317)^+ \to D_s^+\pi^0$ and $D_{sJ}(2460)^+ \to D_s^+\pi^0\gamma$ reflections, there is considerable uncertainty in the potential amount of $D_{sJ}^*(2317)^+ \to D_s^+\gamma$ decays.

The likelihood fit represents the background by a constant plus the tail of a Gaussian distribution. The result of the fit is shown in Fig. 4. A $D_{sJ}(2460)^+$ mass of $[2457.2 \pm 1.6]$ MeV/c^2 and

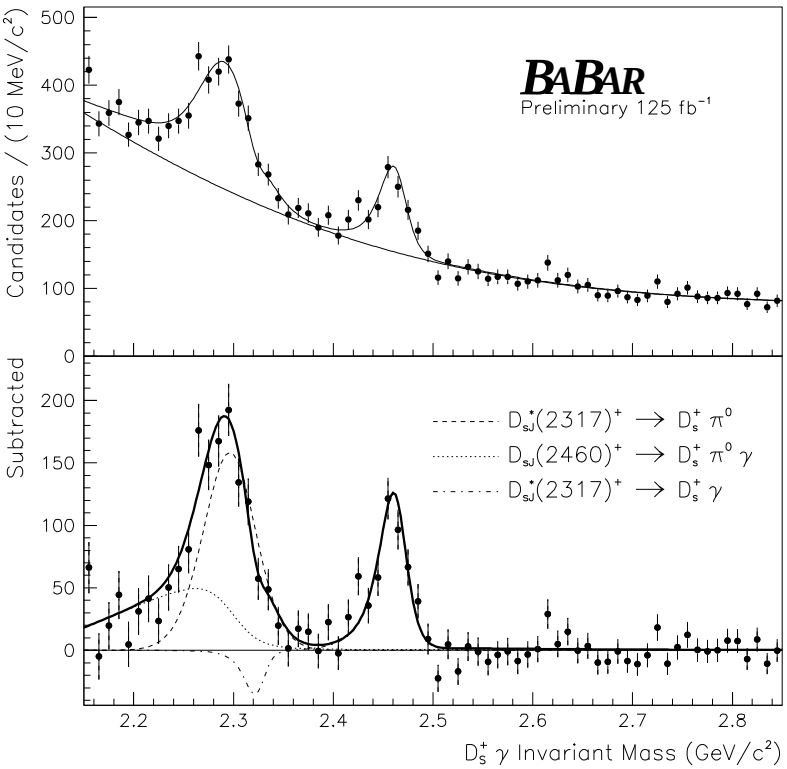

Figure 4: (top) The $D_s^+\gamma$ invariant mass distribution for candidates that satisfy the requirements discussed in the text. The solid curve is the result of a unbinned likelihood fit. (bottom) The mass distribution after subtracting the contribution from combinatorial background as estimated by the fit. Various contributions to the signal and reflection portions of the fit are overlaid. The $D_{sJ}^*(2317)^+$ signal (dot-dash line) appears as a negative contribution due to a negative fluctuation in the fit.

yield of 509 ± 46 mesons is obtained (statistical errors only). The fit, which allows the signal yield to fluctuate to negative values, obtains -107 ± 84 $D_{sJ}^*(2317)^+$ decays (statistical errors only).

The largest uncertainty in the likelihood fit is the shape of the reflection and background. Any tails in the signal or reflection mass distributions will tend to fill in the region of mass around 2.35 MeV/c^2, suppressing the size of the background and inflating signal yields. In addition, as mentioned above, the $D_{sJ}^*(2317)^+$ yield is sensitive to the shape of the reflections because the two peaks overlap. In particular, if the Monte Carlo predictions for the reflect shape and size is used in the fit, the $D_{sJ}^*(2317)^+$ yield is increased to 209 mesons.

Another systematic check is to use alternate functions to describe the combinatorial background, in which case it is possible to change the $D_{sJ}(2460)^+$ yield by at most 3% without adversely affecting the fit quality.

6 THE $D_s^+\pi^0\gamma$ SYSTEM

A likelihood fit to the $D_s^+\pi^0\gamma$ invariant mass distribution is used to determine the mass and yield of the $D_{sJ}(2460)^+$ meson. Because this is a three body decay, there are additional issues that need to be addressed. In particular, it is reasonable to assume that the $D_{sJ}(2460)^+$ decays to $D_s^+\pi^0\gamma$ through either of two possible intermediate resonances: $D_s^*(2112)^+\pi^0$ or $D_{sJ}^*(2317)^+\gamma$. As shown in Fig. 3, these two decay modes overlap in all three mass projections. There is no *a priori* reason to favor one decay path over another. A second, two-dimensional fit is used to distinguish them.

To select the data sample for studying the $D_{sJ}(2460)^+$ meson, the quantity $Q' = S/\sqrt{S+B}$ is optimized simultaneously for both the minimum π^0 momentum and γ energy. The expected signal size S is calculated based on results from previous measurements [5]. Based on this procedure a minimum π^0 momentum of 400 MeV/c and minimum γ energy of 135 MeV is chosen.

Included in Fig. 5 is the $D_s^+\pi^0\gamma$ mass spectrum for all selected candidates below a mass of 2.75 GeV/c^2. A peak near the $D_{sJ}(2460)^+$ mass is apparent. The signal shape of the $D_{sJ}(2460)^+$ is obtained by fitting a signal Monte Carlo sample. This shape is combined with a second order polynomial to fit the mass spectrum. The result is a $D_{sJ}(2460)^+$ mass of $[2457.8 \pm 2.8]$ MeV/c^2 and yield of 246 ± 44 mesons (statistical errors only). The $D_{sJ}(2460)^+$ peak, however, is underlayed by a substantial background which has structure that is not well represented by a simple polynomial. To obtain a more accurate measurement of the $D_{sJ}(2460)^+$ meson requires a more refined selection to isolate the signal.

Since both the $D_s^*(2112)^+\pi^0$ and $D_{sJ}^*(2317)^+\gamma$ decay modes are restricted to a $D_s^+\gamma$ mass near the $D_s^*(2112)^+$ mass, the $D_{sJ}(2460)^+$ signal can be isolated by requiring the $D_s^+\gamma$ invariant mass to reside within 2 MeV/c^2 of the $D_s^*(2112)^+$ mass (2112.4 MeV/c^2 [7]). The result is included in Fig. 5. Although the background is now substantially reduced, it is clear that some type of peaking background has been introduced by this requirement since the size of the peak in the restricted data sample is noticeably larger than that of the inclusive sample.

The source of the peaking background can be investigated further by considering two $D_s^*(2112)^+$ sidebands, each of total width 40 MeV/c^2 in $D_s^+\gamma$ mass and with centers separated by ± 60 MeV/c^2 from the $D_s^*(2112)^+$ mass. The $D_s^+\pi^0\gamma$ mass distribution in these sidebands is included in Fig. 6. Two reflections are observed. Both can be identified in the $D_s^+\pi^0$ invariant mass distribution of Fig. 2. The peak that appears near a $D_s^+\pi^0\gamma$ mass of 2.25 MeV/c^2 in the lower $D_s^+\gamma$ sideband originates from $D_s^*(2112)^+ \to D_s^+\gamma$ decays combined with two unassociated γ particles, one of which has been combined with the γ from the $D_s^*(2112)^+$ decay to form a fake π^0 candidate. A calculation of kinematics based only on the D_s^+, π^0, and $D_{sJ}(2460)^+$ masses can demonstrate that

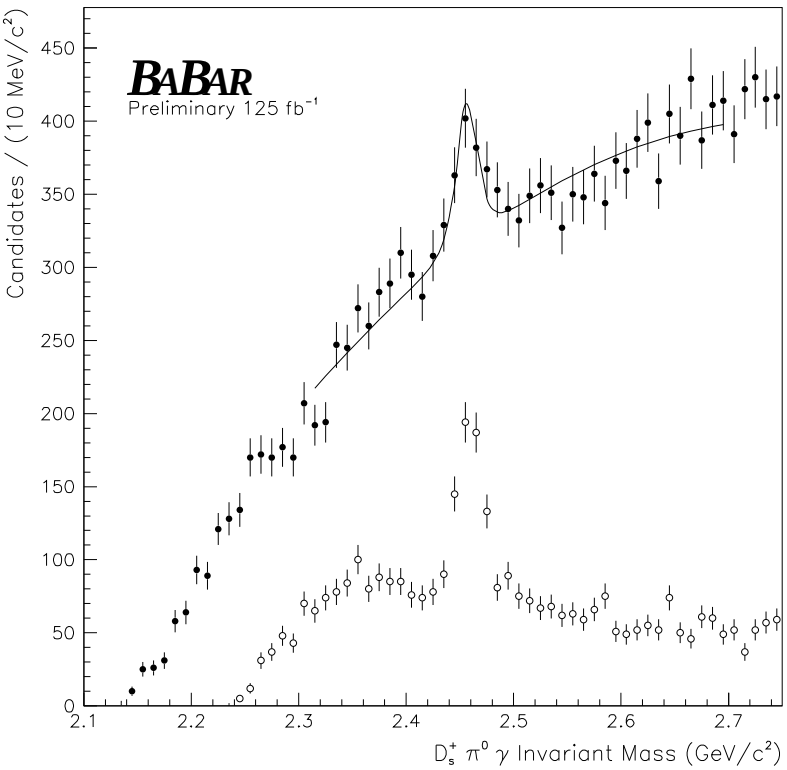

Figure 5: The inclusive and semi-inclusive $D_s^+\pi^0\gamma$ invariant mass distributions. Shown in solid points is the total data sample. Overlaid is the simple line fit discussed in the text. Shown in open round points is the subset which has a $D_s^+\gamma$ mass within ± 2 MeV/c^2 of the $D_s^*(2112)^+$ mass.

the $D_s^*(2112)^+$ reflection will appear with a predictable amount of smearing at a specific $D_s^+\pi^0\gamma$ mass in the $D_s^+\gamma$ signal and sideband selections.

A more important reflection is from $D_{sJ}^*(2317)^+ \to D_s^+\pi^0$ decays combined with unassociated γ particles. The position and lineshape of this reflection has been determined using $D_{sJ}^*(2317)^+$ Monte Carlo. Although the Monte Carlo prediction of the size of the reflection is consistent with the data within statistics, its size has been adjusted uniformly upwards by 23% (corresponding to approximately one standard deviation) to best match the amplitudes observed in the two $D_s^+\gamma$ sidebands. The accuracy of the Monte Carlo prediction of the $D_{sJ}^*(2317)^+$ shape has already been confirmed in the $D_s^+\pi^0$ fit shown in Fig. 2

Independent likelihood fits are applied to each of the sideband distributions and to the signal distribution. All three fits can successfully model their respective data samples, as shown in Fig. 6. The fit to the $D_s^+\gamma$ signal region includes those two reflections and the $D_{sJ}(2460)^+$ signal. The $D_{sJ}(2460)^+$ mass is included in the fit by allowing the lineshape to up or down in mass. The fit obtains a $D_{sJ}(2460)^+$ mass of $[2459.1 \pm 1.3]$ MeV/c^2 and yield of 292 ± 29 mesons (statistical errors only).

A systematic uncertainty specific to this fit is the size of the $D_{sJ}^*(2317)^+$ reflection. Using the prediction of yield from the Monte Carlo unchanged increases the $D_{sJ}(2460)^+$ yield to 308 mesons and shifts the mass upwards by 0.3 MeV/c^2.

The fit of the $D_s^+\pi^0\gamma$ mass does little to differentiate between the two possible $D_{sJ}(2460)^+$ decay modes $D_s^*(2112)^+\pi^0$ and $D_{sJ}^*(2317)^+\gamma$. It is necessary for this purpose to investigate the $D_s^+\pi^0$ and $D_s^+\gamma$ mass distributions more closely. As shown in Fig. 3, the $D_s^*(2112)^+\pi^0$ decay can be expected to appear as a sharp peak in the $D_s^+\gamma$ spectrum centered on the $D_s^*(2112)^+$ mass, and with a distribution spread out by approximately 41.3 MeV/c^2 in $D_s^+\pi^0$ mass centered at 2313.4 MeV/c^2. In contrast, the decay $D_{sJ}(2460)^+ \to D_{sJ}^*(2317)^+\gamma$ appears as a sharp peak in the $D_s^+\pi^0$ spectrum and as a distribution spead out by approximately 40.9 MeV/c^2 in the $D_s^+\gamma$ spectrum centered at 2110.5 MeV/c^2.

The $D_s^+\pi^0$ and $D_s^+\gamma$ mass distributions of the signal cannot be explored without correctly subtracting backgrounds from $D_s^*(2112)^+ \to D_s^+\gamma$ and $D_{sJ}^*(2317)^+ \to D_s^+\pi^0$ decays. This subtraction is performed by a two-dimensional unbinned likelihood applied to the $D_s^+\pi^0$ and $D_s^+\gamma$ mass distributions of the data. The likelihood fit is restricted to the data sample contained in the boundaries illustrated in Fig. 7. This fit includes five sources of $D_s^+\pi^0\gamma$ candidates:

- Combinatorial background represented by a two-dimensional quadratic function.
- Background from $D_s^*(2112)^+ \to D_s^+\gamma$ decays combined with unassociated π^0 candidates represented by a $D_s^*(2112)^+$ lineshape in the $D_s^+\gamma$ mass and as a linear function in $D_s^+\pi^0$ mass.
- Background from $D_{sJ}^*(2317)^+ \to D_s^+\pi^0$ decays combined with unassociated γ candidates represented by a $D_{sJ}^*(2317)^+$ lineshape in the $D_s^+\pi^0$ mass and as a linear function in $D_s^+\gamma$ mass.
- A signal from $D_{sJ}(2460)^+ \to D_s^*(2112)^+\pi^0$ represented by a $D_s^*(2112)^+$ lineshape in the $D_s^+\gamma$ mass and a 41.5 MeV/c^2 wide reflection in the $D_s^+\pi^0$ mass with a specific shape and mass predicted by signal Monte Carlo.
- A signal from $D_{sJ}(2460)^+ \to D_{sJ}^*(2317)^+\gamma$ represented by a $D_{sJ}^*(2317)^+$ lineshape in the $D_s^+\pi^0$ mass and a 40.9 MeV/c^2 wide reflection in the $D_s^+\gamma$ mass with a shape determined from kinematics smeared by a resolution extracted from signal Monte Carlo.

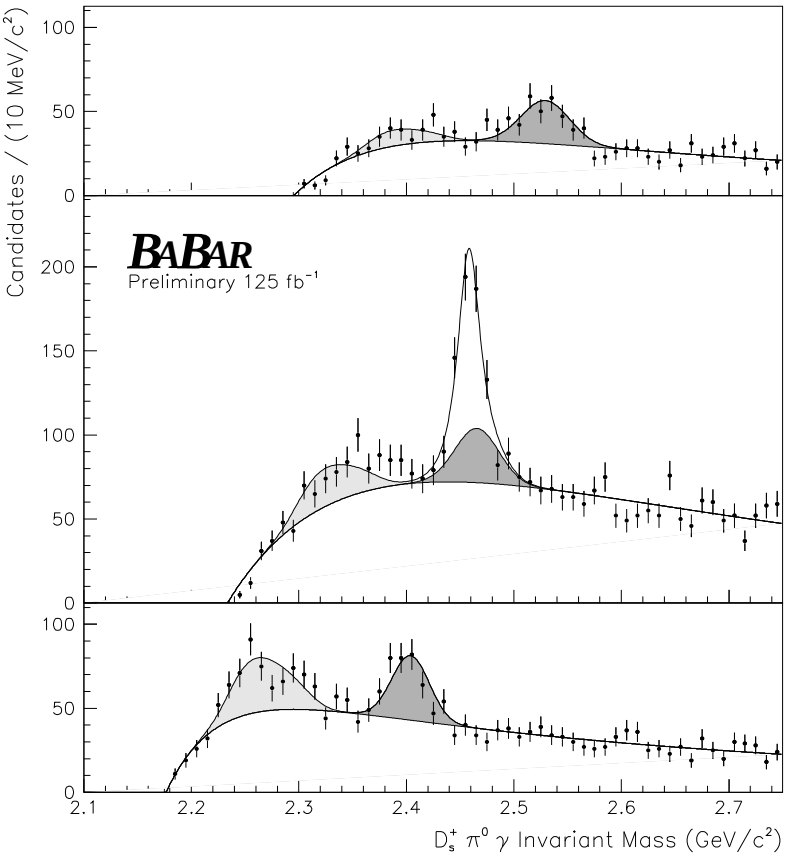

Figure 6: The $D_s^+\pi^0\gamma$ mass spectrum of the sample of events that fall in a $D_s^+\gamma$ signal region (center plot), the $D_s^+\gamma$ high mass sideband (top plot), and the low mass sideband (bottom plot). The $D_{sJ}(2460)^+$ signal appears only in the signal region. The results of separate likelihood fits are superimposed on all three distributions. Reflections from (dark gray) $D_{sJ}^*(2317)^+ \to D_s^+\pi^0$ and (light gray) $D_s^*(2112)^+ \to D_s^+\gamma$ decays appear in all three distributions at positions that are fixed from kinematics. The relative contribution of the $D_{sJ}^*(2317)^+$ reflection in each sample has been determined using signal Monte Carlo.

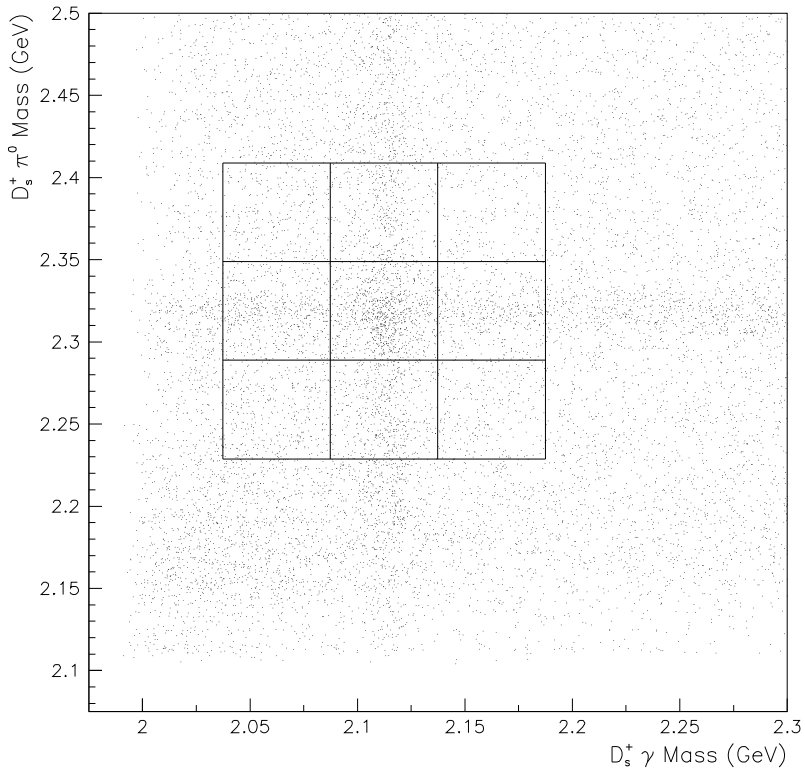

Figure 7: A scatter plot of the $D_s^+\pi^0$ versus $D_s^+\gamma$ invariant masses from the sample of $D_s^+\pi^0\gamma$ candidates. Two bands from $D_{sJ}^*(2317)^+ \to D_s^+\pi^0$ and $D_s^*(2112)^+ \to D_s^+\gamma$ decays are clearly visible as background. The $D_{sJ}(2460)^+$ signal consists of an excess of candidates near the area these two bands cross. The grid lines indicate the range of events used in a likelihood fit.

The results of this likelihood fit is shown in Fig. 8, divided into the regions delineated by the grid shown in Fig. 7. The fit produces an adequate model of the data in all regions. The result (statistical errors only) is a $D_s^*(2112)^+\pi^0$ yield of 266 ± 38 mesons and a $D_{sJ}^*(2317)^+\gamma$ yield of -11 ± 37 mesons, the former number being somewhat smaller than the yield determined by the first fit, though consistent within systematic uncertainties. Based on these results, it appears that the decay $D_{sJ}(2460)^+ \to D_s^+\pi^0\gamma$ can be successfully described as proceeding entirely through the channel $D_s^*(2112)^+\pi^0$.

The likelihood fit of Fig. 8 is sensitive to various assumptions. For example, the $D_{sJ}^*(2317)^+\gamma$ yield can be raised to 2 candidates while preserving the quality of the fit if the mass resolutions are degraded slightly. In addition, possible inaccuracies in the inclusive $D_s^*(2112)^+$ p^* distribution predicted by Monte Carlo can produce changes in the $D_s^*(2112)^+$ lineshape that can raise the yield of $D_s^*(2112)^+\pi^0$ decays to 280.

7 THE $D_s^+\pi^+\pi^-$ SYSTEM

To form $D_s^+\pi^+\pi^-$ candidates, each D_s^+ is combined with π^+ and π^- candidates with momentum above 250 MeV/c. This momentum requirement is obtained from the optimization of Q for the decay $D_{sJ}(2460)^+ \to D_s^+\pi^+\pi^-$. The resulting invariant mass distribution has two distinct, narrow peaks, as shown in Fig. 9. These two peaks correspond to the decays of the $D_{sJ}(2460)^+$ and $D_{s1}(2536)^+$ mesons, as previously noted by the BELLE collaboration [3].

There is a type of reflection that could be introduced into the inclusive distribution of $D_s^+\pi^+\pi^-$ mass that would not appear in the other combinations discussed up to this point. An example of such a reflection is the hypothetical decay of a heavy particle into ϕ or K^* plus two charged particles, either of which might be a K meson or proton. The corresponding ϕ or K^* from this decay can be combined with an unassociated π^+ candidate to form a fictitious D_s^+ candidate. The result could produce a peak in the $D_s^+\pi^+\pi^-$ mass distribution when combined with the other decay products. As a sanity check, the D_s^+ decay products are combined with the $\pi^\pm$ candidates using various different particle species hypotheses ($\pi^\pm$, p, $K^\pm$) to check for underlying resonances not associated with D_s^+ decay. No such resonances are uncovered.

The likelihood fit to the $D_s^+\pi^+\pi^-$ mass distribution consists of three signal distributions ($D_{sJ}^*(2317)^+$, $D_{sJ}(2460)^+$, or $D_{s1}(2536)^+$ decay) plus a third-order polynomial to describe the combinatorial background. The shapes of the three signals are derived from signal Monte Carlo samples. The $D_{sJ}(2460)^+$ and $D_{s1}(2536)^+$ signal shapes are allowed to shift upwards and downwards in mass in order to best describe the data. The result of this fit, included in Fig. 9, is (statistical errors only) a $D_{sJ}^*(2317)^+$ yield of 0.6 ± 1.8 decays; a $D_{sJ}(2460)^+$ mass and yield of $[2460.1 \pm 0.3]$ MeV/c^2 and 67 ± 11 decays; and a $D_{s1}(2536)^+$ mass and yield of $[2534.3 \pm 0.4]$ MeV/c^2 and 124 ± 18 decays.

A systematic uncertainty specific to this likelihood fit is the assumption of the background shape. Substituting a fourth-order polynomial for the background changes the $D_{sJ}(2460)^+$ and $D_s^*(2112)^+$ yields by a relative 5.3% and 9.1%.

8 THE $D_s^+\pi^\pm$ SYSTEM

There has been some conjecture [9, 10, 11] that the $D_{sJ}^*(2317)^+$ may be a four-quark hybrid state. It might be expected, if this was true, that neutral and doubly-charged partners should exist with a similar mass. The $D_s^+\pi^\pm$ system can be used to test this possibility.

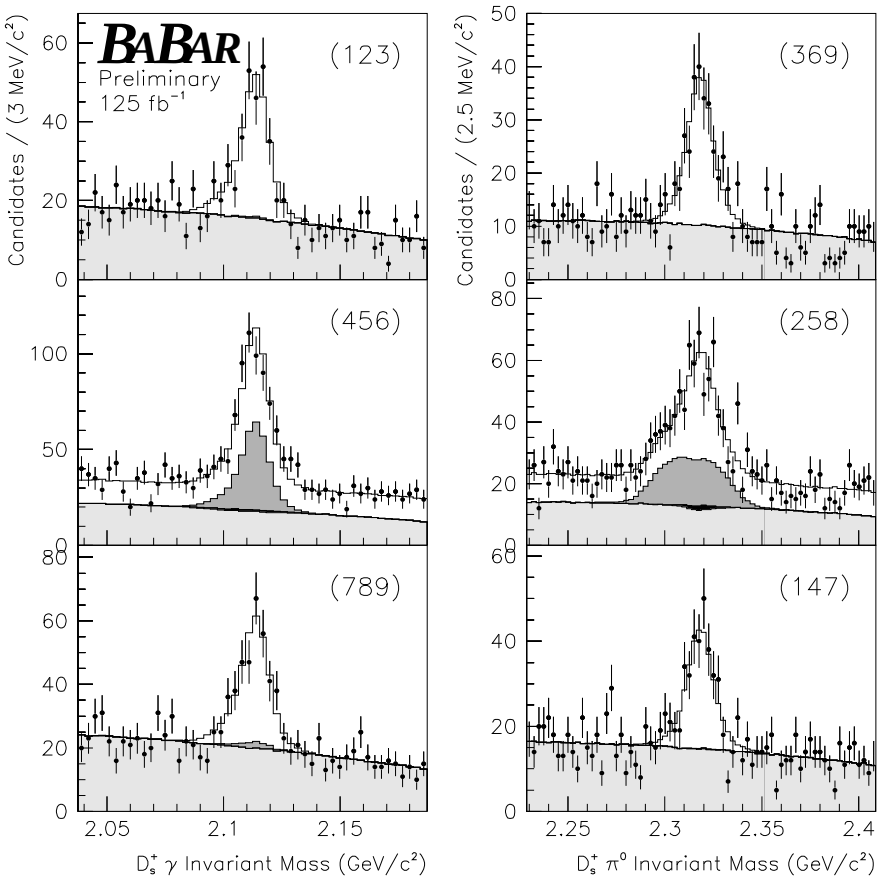

Figure 8: The results of a likelihood fit to the $D_s^+\pi^0$ and $D_s^+\gamma$ masses of the $D_s^+\pi^0\gamma$ candidates which appear inside the grid shown in Fig. 7. Each plot corresponds to a column or row of that grid as indicated by the numbers in parentheses. The points correspond to the data. The histograms are a Monte Carlo representation of the fit results. Shown in gray (black) are the contributions from $D_{sJ}(2460)^+ \to D_s^*(2112)^+\pi^0$ ($D_{sJ}(2460)^+ \to D_{sJ}^*(2317)^+\gamma$) decay predicted by the fit. The light gray area is the contribution from combinatorial background.

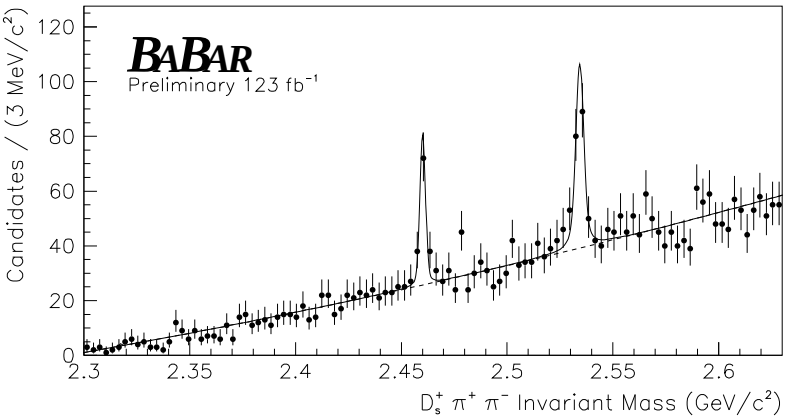

Figure 9: The $D_s^+\pi^+\pi^-$ invariant mass distribution for candidates that satisfy the requirements discussed in the text. The solid curve is the result of a unbinned likelihood fit.

To form $D_s^+\pi^\pm$ combinations, each D_s^+ candidate is combined with $\pi^\pm$ candidates with momentum greater than 300 MeV/c. This momentum requirement is obtained from the optimization of Q for the hypothetical decay $D_{sJ}^*(2317)^0 \to D_s^+\pi^-$. The resulting mass distributions are shown in Fig. 10. No resonant structure is observed.

Likelihood fits have been performed assuming a hypothetical $D_{sJ}^*(2317)^0$ or $D_{sJ}^*(2317)^{++}$ state at precisely the $D_{sJ}^*(2317)^+$ mass. The results of these fits are included in Fig. 10. The yields obtained for the fit (statistical errors only) for the $D_{sJ}^*(2317)^0$ and $D_{sJ}^*(2317)^{++}$ are -28 ± 25 and -39 ± 16 mesons, respectively.

9 SYSTEMATIC STUDIES

There are various systematic uncertainties in common to many of the likelihood fits presented here. As discussed earlier, there is an uncertainty of ± 0.6 MeV/c^2 in the given D_s^+ mass. A 1% uncertainty in the energy calibration of the EMC results in uncertainties of between 0.6 and 0.8 MeV/c^2 for those combinations which include a π^0 or γ candidate. The largest uncertainty in the $\pi^\pm$ momentum arises from the accuracy of the calculations applied by the track reconstruction software to account for the energy loss in the material of the detector. A conservative estimate of the effect on the $D_s^+\pi^+\pi^-$ mass of all tracking uncertainties is ± 1 MeV/c^2.

The mass lineshapes used in the likelihood fits of this analysis, derived from Monte Carlo simulation, provide models of the data of satisfactory quality. Variations in the resolution of the detector have been applied to widen these lineshapes within reasonable bounds. The resulting change in yield or mass is assigned as a systematic uncertainty.

As mentioned earlier, the reconstruction efficiency for all particle combinations discussed in this paper vary as a function of p^*. Yields are calculated by performing separate likelihood fits with candidates weighted by the inverse of this efficiency. To check this approach, likelihood fits are also performed on the candidate sample divided into bins of p^*. The yields from the binned data are calculated using the average reconstruction efficiency in that bin. Any difference in yield produced by these two methods is assigned as a systematic uncertainty.

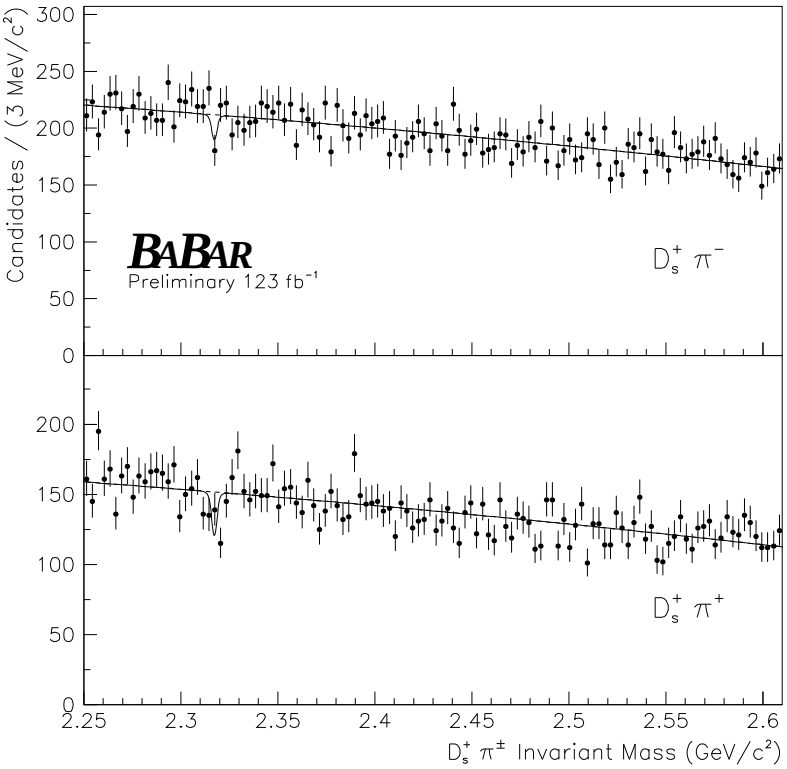

Figure 10: The $D_s^+\pi^-$ (top) and $D_s^+\pi^+$ (bottom) invariant mass distributions for candidates that satisfy the requirements discussed in the text. The solid curve is the result of a unbinned likelihood fit.

Any inaccuracies in the Monte Carlo predictions of the reconstruction efficiency will affect the calculation of branching ratios. As already discussed, the uncertainty in π^0 or γ efficiency is assumed to be 3% and the uncertainty in tracking efficiency is assumed to be 1.3%.

10 COMBINED RESULTS

A preliminary measurement of the $D_{sJ}^*(2317)^+$ mass has been obtained from the $D_s^+\pi^0$ system:

$$m(D_{sJ}^*(2317)^+) = 2318.9 \pm 0.3 \text{ (stat.)} \pm 0.9 \text{ (syst.) MeV/c}^2 . \quad (1)$$

Preliminary measurements of the $D_{sJ}(2460)^+$ has been obtained from $D_s^+\gamma$, $D_s^+\pi^0\gamma$, and $D_s^+\pi^+\pi^-$ decays. The results, in units of MeV/c^2, are:

$$\begin{aligned} m(D_{sJ}(2460)^+ \to D_s^+\gamma) &= 2457.2 \pm 1.6 \text{ (stat.)} \pm 1.3 \text{ (syst.)} & (2)\\ m(D_{sJ}(2460)^+ \to D_s^+\pi^0\gamma) &= 2459.1 \pm 1.3 \text{ (stat.)} \pm 1.2 \text{ (syst.)} & (3)\\ m(D_{sJ}(2460)^+ \to D_s^+\pi^+\pi^-) &= 2460.1 \pm 0.3 \text{ (stat.)} \pm 1.2 \text{ (syst.)} . & (4) \end{aligned}$$

The average of these results, after accounting for correlated systematic uncertainties, is:

$$m(D_{sJ}(2460)^+) = 2459.4 \pm 0.3 \text{ (stat.)} \pm 1.0 \text{ (syst.) MeV/c}^2 . \quad (5)$$

The fit to the $D_s^+\pi^+\pi^-$ mass spectrum also provides a preliminary estimate of the $D_{s1}(2536)^+$ mass:

$$m(D_{s1}(2536)^+) = 2534.3 \pm 0.4 \text{ (stat.)} \pm 1.2 \text{ (syst.) MeV/c}^2 . \quad (6)$$

The following preliminary branching ratios have been estimated by comparing the efficiency corrected yields from the corresponding decay modes.

$$\frac{\mathcal{B}r(D_{sJ}(2460)^+ \to D_s^+\gamma)}{\mathcal{B}r(D_{sJ}(2460)^+ \to D_s^+\pi^0\gamma)} = 0.375 \pm 0.054 \text{ (stat.)} \pm 0.057 \text{ (syst.)} \quad (7)$$

$$\frac{\mathcal{B}r(D_{sJ}(2460)^+ \to D_s^+\pi^+\pi^-)}{\mathcal{B}r(D_{sJ}(2460)^+ \to D_s^+\pi^0\gamma)} = 0.082 \pm 0.018 \text{ (stat.)} \pm 0.011 \text{ (syst.)} \quad (8)$$

A 95% CL upper limit has been calculated for the decay modes in which no significant signal is observed. This limit is based on the deviation from the measured yields of 1.96 standard deviations, derived from the quadrature sum of statistical and systematic uncertainties.

$$\frac{\mathcal{B}r(D_{sJ}^*(2317)^+ \to D_s^+\gamma)}{\mathcal{B}r(D_{sJ}^*(2317)^+ \to D_s^+\pi^0)} < 0.17 \quad (9)$$

$$\frac{\mathcal{B}r(D_{sJ}(2460)^+ \to D_s^+\pi^0)}{\mathcal{B}r(D_{sJ}(2460)^+ \to D_s^+\pi^0\gamma)} < 0.11 \quad (10)$$

$$\frac{\mathcal{B}r(D_{sJ}(2460)^+ \to D_{sJ}^*(2317)^+\gamma)}{\mathcal{B}r(D_{sJ}(2460)^+ \to D_s^+\pi^0\gamma)} < 0.23 \quad (11)$$

$$\frac{\mathcal{B}r(D_{sJ}^*(2317)^+ \to D_s^+\pi^+\pi^-)}{\mathcal{B}r(D_{sJ}^*(2317)^+ \to D_s^+\pi^0)} < 2 \cdot 10^{-3} \quad (12)$$

11 CONCLUSION

Based on 125 fb^{-1} of $e^+e^- \to c\overline{c}$ data, the $D^*_{sJ}(2317)^+$ and $D_{sJ}(2460)^+$ masses are measured to be [2318.9$\pm$0.3 (stat.)$\pm$0.9 (syst.)] MeV/c^2 and [2459.4$\pm$0.3 (stat.)$\pm$1.0 (syst.)] MeV/c^2, respectively. Both values are consistent with previous measurements [2, 3, 4] with perhaps the exception of the $D^*_{sJ}(2317)^+$ mass which is 1.6 MeV/c^2 higher than our previous result [5].

Significant signals are observed for $D^*_{sJ}(2317)^+ \to D_s^+\pi^0$, $D_{sJ}(2460)^+ \to D_s^+\gamma$, $D_{sJ}(2460)^+ \to D_s^+\pi^0\gamma$, and $D_{sJ}(2460)^+ \to D_s^+\pi^+\pi^-$. The data is consistent with the $D_{sJ}(2460)^+ \to D_s^+\pi^0\gamma$ decay proceeding entirely through the channel $D_s^*(2112)^+\pi^0$. The $D_s^+\pi^+\pi^-$ result confirms the decay first observed by Belle [3], although at a rate that is somewhat lower.

No significant signal is observed for either the $D_s^+\gamma$ or $D_s^+\pi^+\pi^-$ decays of the $D^*_{sJ}(2317)^+$. A search for the $D_s^+\pi^0$ decay of the $D_{sJ}(2460)^+$ also produces no significant signal. Searches for a neutral or doubly-charged partner for the $D^*_{sJ}(2317)^+$ decaying to $D_s^+\pi^+$ or $D_s^+\pi^-$ also produce no significant signal.

ACKNOWLEDGMENTS

We are grateful for the extraordinary contributions of our PEP-II colleagues in achieving the excellent luminosity and machine conditions that have made this work possible. The success of this project also relies critically on the expertise and dedication of the computing organizations that support *BABAR*. The collaborating institutions wish to thank SLAC for its support and the kind hospitality extended to them. This work is supported by the US Department of Energy and National Science Foundation, the Natural Sciences and Engineering Research Council (Canada), Institute of High Energy Physics (China), the Commissariat à l'Energie Atomique and Institut National de Physique Nucléaire et de Physique des Particules (France), the Bundesministerium für Bildung und Forschung and Deutsche Forschungsgemeinschaft (Germany), the Istituto Nazionale di Fisica Nucleare (Italy), the Foundation for Fundamental Research on Matter (The Netherlands), the Research Council of Norway, the Ministry of Science and Technology of the Russian Federation, and the Particle Physics and Astronomy Research Council (United Kingdom). Individuals have received support from CONACyT (Mexico), the A. P. Sloan Foundation, the Research Corporation, and the Alexander von Humboldt Foundation.

References

[1] *BABAR* Collaboration, B. Aubert *et al.*, Phys. Rev. Lett. **90**, 242001 (2003).

[2] CLEO Collaboration, D. Besson *et al.*, Phys. Rev. **D68**, 032002 (2003).

[3] BELLE Collaboration, K. Abe *et al.*, Phys. Rev. Lett. **92**, 012002 (2004).

[4] BELLE Collaboration, P. Krokovny *et al.*, Phys. Rev. Lett. **91**, 262002 (2003).

[5] *BABAR* Collaboration, B. Aubert *et al.*, Phys. Rev. **D69**, 031101 (2004).

[6] *BABAR* Collaboration, B. Aubert *et al.*, Nucl. Instr. Meth. **A479**, 1 (2002).

[7] Particle Data Group Collaboration, K. Hagiwara *et al.*, Phys. Rev. **D66**, 010001 (2002).

[8] GEANT4 Collaboration, S. Agostinelli *et al.*, Nucl. Instr. Meth. **A506**, 250 (2003).

[9] T. Barnes, F. E. Close, and H. J. Lipkin, Phys. Rev. **D68**, 054006 (2003).

[10] H. J. Lipkin, Phys. Lett. **B580**, 50 (2004).

[11] T. E. Browder, S. Pakvasa, and A. A. Petrov, Phys. Lett. **B578**, 365 (2004).